

## Preclinical MRI Reveals Bevacizumab Mitigates Radiation Necrosis

X Jiang<sup>1</sup>, JA Engelbach<sup>2</sup>, J Cates<sup>3</sup>, DK Thotala<sup>3</sup>, RE Drzymala<sup>3</sup>, DE Hallahan<sup>3</sup>, JJH Ackerman<sup>1</sup>, and JR Garbow<sup>2</sup>

<sup>1</sup>Chemistry, Washington Univ. in st. louis, st louis, MO, United States, <sup>2</sup>Radiology, Washington Univ. in st. louis, st louis, MO, United States, <sup>3</sup>Radiation Oncology, Washington Univ. in st. louis, st louis, MO, United States

**Target Audience:** Clinicians, biologists, and imaging scientists interested in cancer and its treatment with radiation.

**Purpose:** Bevacizumab (Avastin<sup>®</sup>), a humanized monoclonal antibody that inhibits vascular endothelial growth factor A (VEGF-A), is a powerful anti-angiogenic used in the treatment of tumors. Radiation necrosis, a severe but late occurring injury to normal tissue within and surrounding a radiation treatment field, has been described as a slow, continuous process in which increased levels of VEGF-A lead to breakdown of the blood brain barrier [1]. Thus, blocking VEGF-A from reaching capillaries and repair of “leaky” capillaries is a possible therapeutic strategy for radiation necrosis. Recently, a novel mouse model of radiation necrosis that accurately recapitulates the histologic features of radiation necrosis was developed in our laboratory [2]. This animal model provides a platform for a wide variety of studies of radiation necrosis,

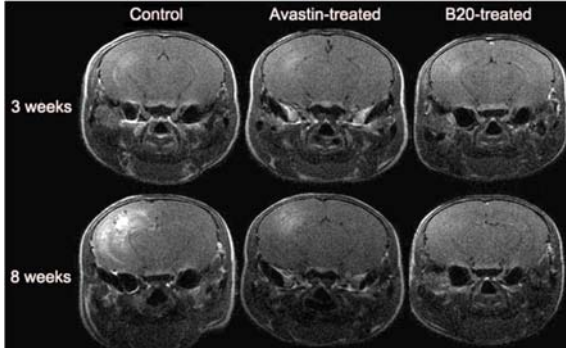


**Figure 1.** Contrast-enhanced T1-weighted MR images of control, Avastin-treated, and B20-4.1.1-treated mice, 3 and 8 weeks post irradiation.

including the potential mitigation of radiation necrosis by bevacizumab. In this work, the therapeutic effect of Avastin and of mouse bevacizumab (B20-4.1.1, Genentech), which is capable of high-affinity binding to both human and murine VEGF-A, are monitored by magnetic resonance imaging. **Methods:** All experiments were approved by the Washington University Division of Comparative Medicine. Hemispheric irradiation of mouse brain was performed with the Leksell Gamma Knife<sup>®</sup> Perfexion<sup>™</sup> (GK), a state-of-the-art unit used for stereotactic irradiation of patients with malignant brain tumors. Three cohorts of 7-8 week old female mice (n=5) were irradiated with a single 60-Gy dose (50% isodose) of GK radiation. At this dose, the onset of radiation necrosis typically occurs 3-4 weeks post-irradiation. Mouse cohort #1 was an irradiated but untreated control; cohort #2 received Avastin (10 mg/kg, twice weekly) from 3-to-10 weeks post-irradiation; cohort #3 received B20-4.1.1 (10 mg/kg, twice weekly) from 3-to-10 weeks post-irradiation. Mice were imaged weekly, from 3-to-10 weeks post-irradiation, using an Agilent/Varian DirectDrive<sup>™</sup> 4.7-T small-animal MR scanner. **Results:** Slices from representative contrast-enhanced, T1-weighted, spin-echo images of control, Avastin-treated and B20-4.1.1-treated mice, collected 3 and 8 weeks post-irradiation, are shown in Fig. 1. It is evident that regions of hyperintensity associated with radiation necrosis progress much more rapidly in the control mouse than in the treated mice. To analyze these data quantitatively, the intensity of each irradiated hemisphere was normalized by the mean intensity of the contralateral/non-irradiated hemisphere, and histograms of normalized intensity were constructed. For non-irradiated, non-treated subjects, the intensity distribution histogram is symmetric, with an intensity range of 0.6-1.4 (data not shown). Thus, voxel intensities greater than 1.4 were taken as identifying necrotic tissue and this threshold was used to define the volume of radiation necrosis. The MRI-derived volumes of radiation necrosis for control, Avastin-treated, and B20-4.1.1-treated mice are plotted in Fig. 2 (left) as a function of time post-irradiation. Differences in necrosis volumes between control and treated mice were statistically significant on week 5 and 6 (P<0.05), clearly demonstrating the mitigative effects of Avastin and B20-4.1.1 during the period 3-7 weeks post-irradiation. The rates of progression of radiation necrosis for the three cohorts, derived from the slope of least-squares fits over the time periods 3-7 and 7-9 weeks post-irradiation, are shown in Fig. 2 (right). It is obvious that in mice, B20-4.1.1 is a more potent mitigator of radiation necrosis than Avastin. **Discussion:** The MRI quantified mitigative effects of Avastin and B20-4.1.1 clearly demonstrates the efficacy of anti-VEGF-A therapy in the treatment of radiation necrosis. The mitigative effect of Avastin disappeared approximately 4 weeks after the start of treatment. This may be due to an immunogenic response whereby murine antibodies directed against the antigen specific

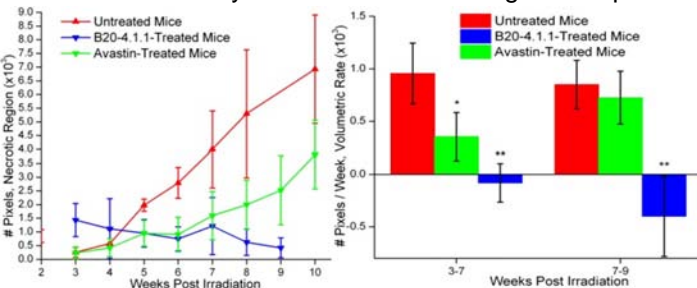


**Figure 2.** (Left) The volume of radiation necrosis vs. time post irradiation for untreated (red), Avastin-treated (green) and B20-4.1.1-treated (blue) mice; (Right) Volumetric rate of radiation necrosis progression, derived from the slope of the curves in the left panel, for the period 3 – 7 and 7 – 9 weeks. \*, Significant difference (P<0.01), \*\*, Significant difference (P<0.005) compared with the untreated group.

Levin V.A., et al. *International Journal of Radiation Oncology Biology Physics* 2011; **79**(5): 1487-1495.

part of “humanized bevacizumab”, are produced, thereby inhibiting its binding to mouse VEGF-A. The greater therapeutic efficacy of B20-4.1.1 (“mouse bevacizumab”) is likely due to its higher affinity for mouse VEGF-A [3]. **Conclusion:** Our data demonstrate a significant mitigative effect of Avastin and B20-4.1.1 in a mouse model of radiation necrosis, an effect also observed recently in a group of brain-tumor patients treated with Avastin [4]. Efforts to verify the mechanism of action of Avastin and B20-4.1.1 in

the treatment of radiation necrosis in the mouse model are ongoing. **References:** (1) Siu A, et al. *Acta Neurochirurgica* 2012; **154**(2): 191-201. (2) Jost SC, et al. *Int J Radiat Oncol Biol Phys* 2009; **75**: 527-33. (3) Yu L.L., et al. *Investigative Ophthalmology&Visual Science* 2008; **49**(2): 522-527. (4)